OPEN ACCESS

University of BRISTOL

Ramlan, R., Brennan, M. J., Kovacic, I., Mace, B. R., & Burrow, S. (2016). Exploiting knowledge of jump-up and jump-down frequencies to determine the parameters of a Duffing oscillator. *Communications in Nonlinear Science and Numerical Simulation*, *37*, 282-291. https://doi.org/10.1016/j.cnsns.2016.01.017

Peer reviewed version

Link to published version (if available):
10.1016/j.cnsns.2016.01.017

Link to publication record in Explore Bristol Research
PDF-document

This is the author accepted manuscript (AAM). The final published version (version of record) is available online via Elsevier at http://www.sciencedirect.com/science/article/pii/S1007570416300041 . Please refer to any applicable terms of use of the publisher.

University of Bristol - Explore Bristol Research
General rights

This document is made available in accordance with publisher policies. Please cite only the published version using the reference above. Full terms of use are available:
http://www.bristol.ac.uk/red/research-policy/pure/user-guides/ebr-terms/

BENEFITS OF KNOWING JUMP-UP AND JUMP-DOWN FREQUENCIES IN A DUFFING OSCILLATOR

Roszaidi Ramlan[1*], Michael J. Brennan[2], Ivana Kovacic[3], Brian R. Mace[4] and Steve Burrow[5]

[1]Faculty of Mechanical Engineering, Universiti Teknikal Malaysia Melaka, Hang Tuah Jaya, 76100 Durian Tunggal, Melaka, Malaysia

[2]Department of Mechanical Engineering, UNESP, Ilha Solteira, SP15385-000 Brazil

[3]Centre of Excellence for Vibro-Acoustic Systems and Signal Processing, Faculty of Technical Sciences, University of Novi Sad, 21125 Novi Sad, Serbia

[4]Department of Mechanical Engineering, University of Auckland, Auckland 1142, New Zealand

[5]Department of Aerospace Engineering, University of Bristol, BS1 1TR Bristol, United Kingdom

*Corresponding author; Telephone: +606 234 6891; Fax: +606 234 6884; Email: roszaidi@utem.edu.my

Abstract: This work concerns the novel application of certain non-linear phenomena – jump frequencies in a base-excited Duffing oscillator. First, approximate analytical expressions are derived for the relationships between the jump-up and jump-down frequencies, the damping ratio and the cubic stiffness coefficient. Then, experimental results, accompanied with the results of numerical simulations, are presented to show how one can benefit from knowing these frequencies.

Keywords: Duffing oscillator; base excitation; jumps, cubic stiffness coefficient; viscous damping coefficient.

1. INTRODUCTION

The appearance of nonlinear phenomena used to be seen as dangerous, with a general tendency to avoid them or control them, and several previous decades have been marked by intensive research efforts directed towards these goals (see, for example, [1-3], and the references cited therein). However, the Nonlinear Dynamics of today is experiencing a profound change of its paradigm as recent investigations have taken a different strategy in which nonlinear phenomena are used to good effects. This strategy has beneficially affected different fields in science and engineering, such as vibration isolation [4, 5], energy harvesting [6, 7], micro- and nano-electro-mechanical systems [8], etc.

The novel application of nonlinear phenomena presented in this paper also contributes to this trend and is related to one of the archetypical nonlinear oscillators – the Duffing oscillator [9], whose restoring force $f(u)$ consists of a linear and cubic term:

$$f(u) = k_1 u \pm k_3 u^3, \tag{1.1}$$

where u is the generalised coordinate, and k_1 and k_3 are the linear and cubic stiffness coefficients, respectively. It is known that this restoring force in an unforced, undamped

oscillator yields a nonlinear relationship between the amplitude of vibration of a typical periodic response and its frequency. When presented graphically, this relationship gives the so-called backbone curve (see Figure 1 and and the dashed-dotted line plotted therein). The backbone curve is bent to the right for the hardening Duffing oscillator, which has a positive cubic nonlinearity in Eq. (1.1) and to the left for the softening Duffing oscillator, defined by a negative cubic nonlinearity in Eq. (1.1). When the Duffing oscillator is forced, the hysteresis phenomenon occurs [9], which is indicated by the arrows shown in Figure 1 on a frequency-amplitude/response curve (FRC) of a hardening Duffing oscillator. The solid and dashed arrows depict that the amplitude of the response changes in a different way when the frequency is increased or decreased. Sudden changes of the amplitude occur from Point *A* to Point *B* (this represents a jump-down), while the jump-up occurs from Point *C* to Point *D*. The corresponding jump frequencies are the boundaries of the region with multiple stable solutions on the branches of the FRC (the solid line in Figure 1 represents the stable branch, and the dashed line the unstable branch). Although the jump phenomena are usually seen as undesirable, this study is to show how one can benefit from knowing the values of the frequencies when these jumps appear. The results presented are the continuation of recent investigations concerned with the derivation of the expressions for the jump-up and jump-down frequencies for externally excited Duffing oscillators [10] and their use for the estimation of certain system parameters in such systems [11], while in this work, these expressions, experimental verification and numerical comparisons are given for a base-excited Duffing oscillator.

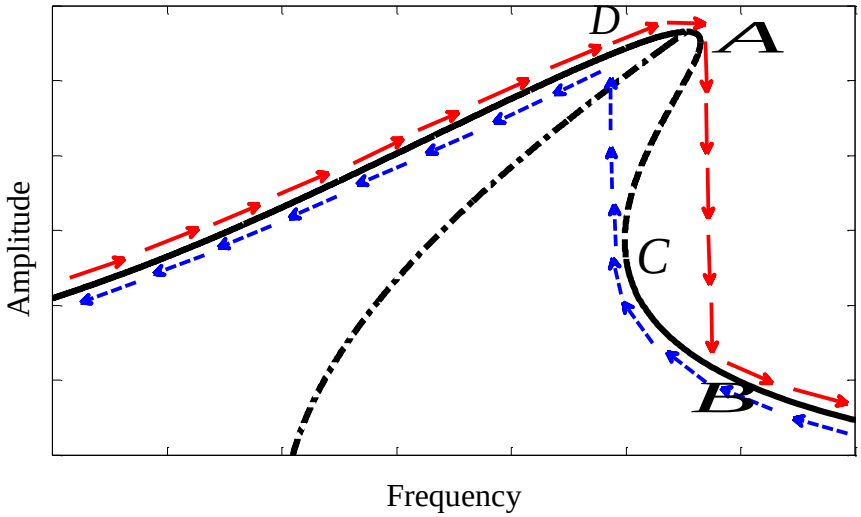

Figure 1. Typical FRC for a hardening Duffing oscillator. The dashed-dotted curve represents the backbone curve, the solid line represents the stable branch, while the dashed line represents the unstable branch.

2. ANALYTICAL APPROACH

Let us consider a damped base-excited Duffing oscillator governed by the following equation of motion:

$$m\ddot{u} + c\dot{u} + f(u) = -m\ddot{z}, \tag{2.1}$$

where m is a mass connected to a parallel combination of a viscous damper with the damping coefficient c and a nonlinear spring the restoring force of which is modelled

by Eq. (1.1). Note that the hardening case is considered here ($k_3 > 0$). The system is excited by a harmonic base displacement $z = Z\cos\omega t$. If $u = x - z$ is the relative displacement between the absolute displacement of the mass x and the base z, Eq. (2.1) can be written in non-dimensional form as

$$\hat{u}'' + 2\zeta\hat{u}' + \hat{u} + \gamma\hat{u}^3 = \Omega^2\cos(\Omega\tau), \tag{2.2}$$

where $\hat{u} = u/Z$ is the non-dimensional relative displacement (relative transmissibility), and where the following substitutions have been introduced: $\gamma = k_3 Z^2/k_1$, $\zeta = c/2m\omega_n$, $\omega_n = \sqrt{k_1/m}$, $\Omega = \omega/\omega_n$, $\tau = \omega_n t$, $(...)' = d(...)/d\tau$. Of particular interest for the subsequent analysis are the cubic stiffness coefficient γ and the damping ratio ζ.

2.1. Approximate expressions for the jump-up and jump-down frequencies

The frequency–amplitude relationship of Eq. (2.2) is computed using the Harmonic Balance method by assuming that the solution to the equation has the form of $\hat{u} = \hat{U}\cos(\Omega\tau + \phi)$ and neglecting the higher harmonics. When the damping is small, such that $\zeta^2 << 1$, the frequency-amplitude relationship is given by

$$\Omega_{1,2} \approx \left(\frac{3\gamma\hat{U}^4 + 4\hat{U}^2 \pm \hat{U}\left(\left(3\gamma\hat{U}^2 + 4\right)^2 - 64\hat{U}^2\zeta^2 - 48\gamma\zeta^2\hat{U}^4\right)^{\frac{1}{2}}}{4\left(\hat{U}^2 - 1\right)} \right)^{\frac{1}{2}}, \tag{2.3}$$

where the subscripts 1 and 2 refer to the resonant and non-resonant branches of the FRC. The expression for the jump-up frequency Ω_u is determined from Eq. (2.3) and the condition of the existence of a vertical tangent $d\Omega_1(\zeta = 0)/d\hat{X} = 0$ [10], which gives

$$\Omega_u \approx 1 + \frac{27}{32}\gamma^{\frac{1}{3}}. \tag{2.4}$$

The jump-down frequency Ω_d is calculated as the one at which two branches of the FRC meet, i.e. when the expression in the middle brackets in Eq. (2.3) is zero. This condition yields the value of $\hat{U}$, which is substituted back in Eq. (2.3) to derive:

$$\Omega_d \approx \frac{1}{\left(1 - \frac{3\gamma}{(4\zeta)^2}\right)^{\frac{1}{2}}}. \tag{2.5}$$

Equations (2.4) and (2.5) imply that the jump-up frequency depends only on the cubic stiffness coefficient and not on the damping ratio, while the jump-down frequency depends on both the cubic stiffness coefficient and the damping ratio. Rearranging and combining Eqs. (2.4) and (2.5) gives the expressions for the nonlinearity and the damping ratio, respectively, as

$$\gamma \approx 2^6\left(\frac{2}{3}\right)^9(\Omega_u - 1)^3, \tag{2.6}$$

$$\zeta \approx 2^{\frac{3}{2}}\left(\frac{2}{3}\right)^{4}\frac{\Omega_d\left(\Omega_u-1\right)^{\frac{3}{2}}}{\left(\Omega_d{}^2-1\right)^{\frac{1}{2}}}. \tag{2.7}$$

Likewise, the estimate of the nonlinearity depends on the jump-up frequency only while the damping ratio is a function of both the jump-up and the jump-down frequencies.

2.2. Sensitivity of stiffness coefficient and damping ratio on the jump frequencies

The jump-down frequency can be obtained experimentally by stepping the excitation frequency from a low frequency to a high frequency in small frequency increments, and vice versa for the jump-up frequency. Inevitably, errors appear in the estimates of these frequencies, which tend to be underestimated because of the system dynamics. The estimated jump-up and jump-down frequencies are given by $\hat{\Omega}_u$ and $\hat{\Omega}_d$ respectively, and the difference between the true and estimated values of the jump-up and jump-down frequencies are given by ξ and ν, respectively. Thus $\hat{\Omega}_u = \Omega_u - \xi$, which results in an estimate of the cubic stiffness coefficient given by

$$\hat{\gamma} \approx 2^{6}\left(\frac{2}{3}\right)^{9}\left[\left(\Omega_u-1\right)-\xi\right]^{3}. \tag{2.8}$$

Expanding and re-arranging Eq. (2.8) yields

$$\hat{\gamma} = \gamma\left[1-\frac{3\xi}{\Omega_u-1}+\frac{3\xi^2}{\left(\Omega_u-1\right)^2}-\frac{\xi^3}{\left(\Omega_u-1\right)^3}\right], \tag{2.9}$$

where γ is the true value of the cubic stiffness coefficient given in Eq. (2.6). It can be seen in Eq. (2.9) that higher powers of ξ are included. These higher terms cannot necessarily be ignored because the denominator $\Omega_u - 1$ may be small compared to 1 for the values used in this study. Thus the estimate of the cubic stiffness coefficient is potentially sensitive to the errors in the estimated jump-up frequency.

Now, $\hat{\Omega}_d = \Omega_d - \nu$, so from Eq. (2.7) the estimated damping ratio, $\hat{\zeta}$ is given by

$$\hat{\zeta} \approx 2^{\frac{3}{2}}\left(\frac{2}{3}\right)^{4}\frac{\left(\Omega_d-\nu\right)\left[\left(\Omega_u-1\right)-\xi\right]^{\frac{3}{2}}}{\left[\left(\Omega_d-\nu\right)^2-1\right]^{\frac{1}{2}}}. \tag{2.10}$$

Factorizing and re-arranging this equation gives

$$\hat{\zeta} = \zeta\frac{\left(\frac{\hat{\Omega}_d}{\Omega_d}\right)\left(1-\frac{\Omega_u-\hat{\Omega}_u}{\Omega_u-1}\right)^{\frac{3}{2}}}{\left(1+\frac{\hat{\Omega}_d{}^2-\Omega_d{}^2}{\Omega_d{}^2-1}\right)^{\frac{1}{2}}}, \tag{2.11}$$

where ζ is the true damping ratio given in Eq. (2.7). This shows that errors in the estimates of the jump-up frequency and the jump-down frequency both result in errors in the estimate of the damping ratio.

3. EXPERIMENTAL INVESTIGATION

This section describes the experimental work carried out to determine the jump-up and jump-down frequency and to further benefit from knowing when they occur. Thus, the method described in the previous section is checked on a nonlinear electromagnetic energy harvesting device [12]. The device is shown in Figure 2(a). It is comprised of two main parts. The first part consists of a steel beam of dimensions width 38.21 mm, thickness 0.5 mm, length 42.70 mm fixed at one end with a mass of 115 g and four magnets attached to the other end. The second part is made up of coil wrapped around an iron core. The arrangement of the magnets on the second part is shown in Figure 2(b).

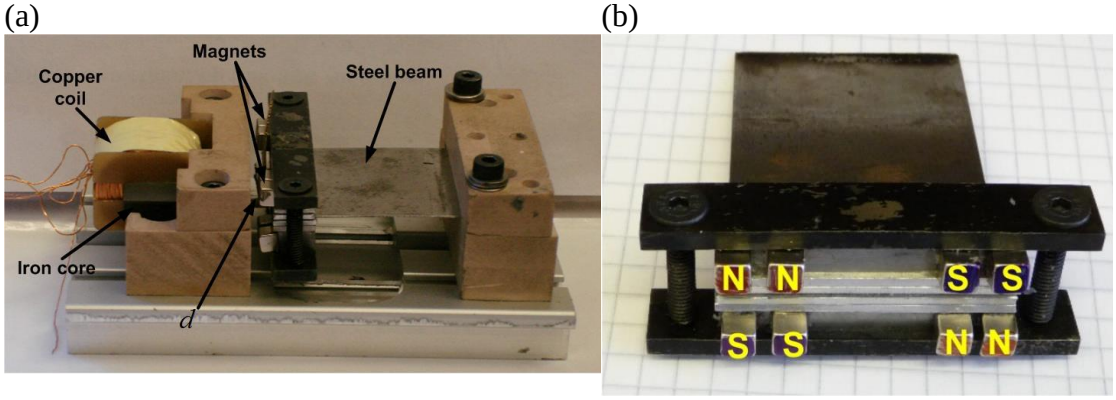

Figure 2. Photographs showing the experimental device: (a) full view and (b) the arrangement of the magnets

This arrangement allows the continuous flow of the magnetic flux between the magnets and the iron core. The total stiffness of the system is the combination of the positive stiffness from the beam and the negative stiffness from the magnets resulting in a nonlinear stiffness characteristic. The two main parts are separated by a gap. The gap *d*, which is shown in Figure 2(a) controls the degree of nonlinearity. When the gap is large the system behaves as a hardening system and when the gap is small the system behaves as a bi-stable system [13]. In this experiment, the gap was set to 1.5 mm so that the system behaved as a hardening system.

3.1. Quasi-static measurement

The stiffness of the system was estimated by a quasi-static measurement as illustrated in Figure 3. This was done by attaching the base of the device to an electro-dynamic shaker which was then driven at a very low frequency. The resulting relative displacement between the tip of the beam and the base was measured using a linear variable differential transformer. The force required to keep the tip of the beam stationary was measured using a force gauge, which was attached to ground.

Figure 4 shows the measured force-deflection plot of the system. The solid curve shows the measured data from the experiment. It can be seen that the plot is not symmetric. This was thought to be due to slight rotation and bending between the connecting arm and the beam. In fitting a polynomial to this curve, symmetry was assumed in which the half cycle where the deflection is positive is mirrored to give a symmetrical curve. This curve was then fitted using the least square method with a cubic polynomial of the Duffing restoring force given by Eq. (1.1), which is shown by

the dashed curve in the figure. The stiffness coefficients were found to be $k_1 = 1495$ N/m and $k_3 = 4.26 \times 10^7$ N/m^3.

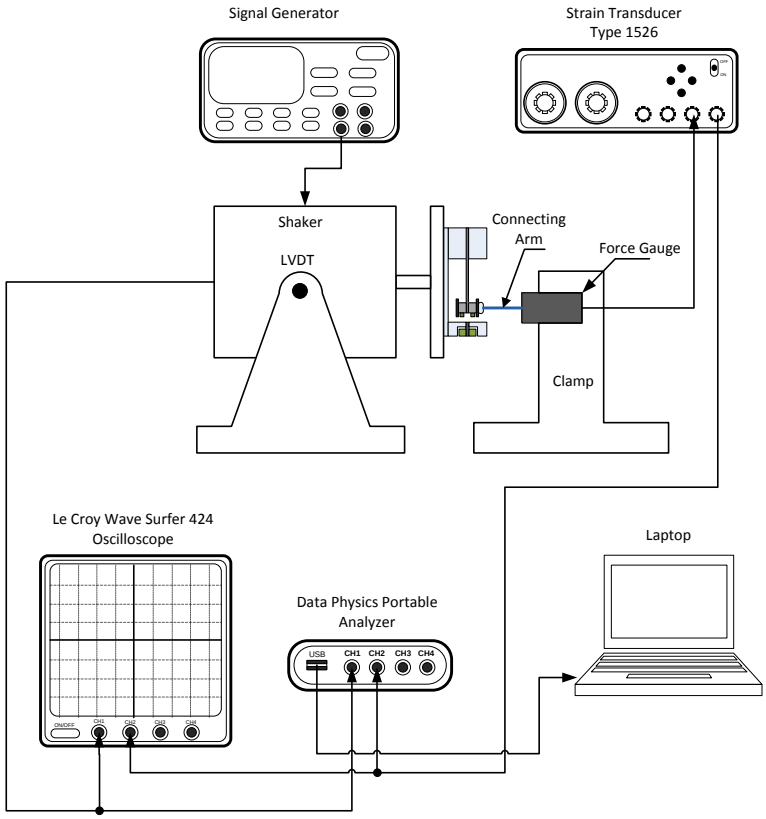

Figure 3. Experimental setup for quasi-static measurement to determine the stiffness.

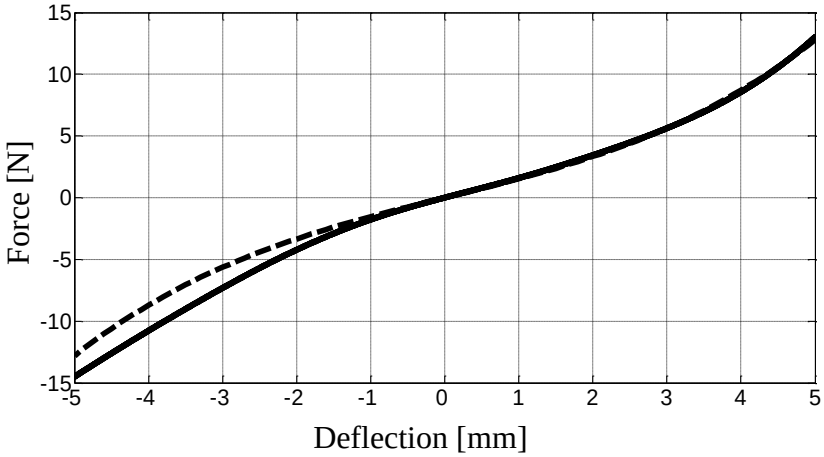

Figure 4. Force-deflection curve: measured (solid) and fitted by assuming that the system is symmetrical (dashed).

3.2.Dynamic measurements

For the dynamic measurements, the whole device was placed onto a shaker so that the system was base-excited and the tip of the beam was free. The experimental setup is shown in Figure 5. The frequency was increased from 15 Hz to 35 Hz in 1 Hz steps and then decreased from 35 Hz to 15 Hz with the same frequency increment. Since the system is nonlinear, the amplitude of the input displacement was maintained at a constant value of 0.1 mm by a feedback controller for all excitation frequencies of interest. The damping in the system was altered by changing the external electrical resistance *R* connected to the coil using a resistor box. The electrical damping is inversely proportional to the resistance, so that the larger the resistance, the smaller the damping. A PCB accelerometer was used to measure the acceleration of the tip mass, which was recorded together with the input displacement for each frequency.

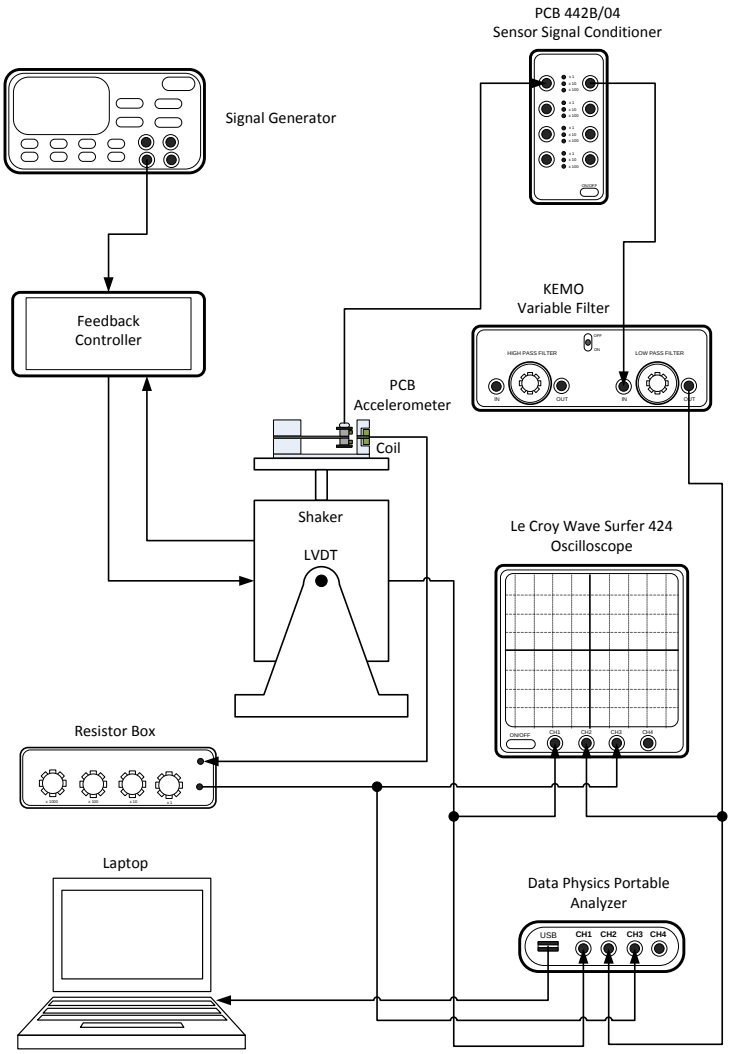

Figure 5. Experimental setup for dynamic measurements.

3.3. Comparison between measurements and numerical simulations

The measured root mean square (rms) displacement for the open-circuit system and that with a 200 Ohm resistance is shown in Figure 6. It can be seen that the jump-down frequencies lie between 29 Hz - 30 Hz and 27 Hz - 28 Hz for the open-circuit system and that with 200 Ohm resistance, respectively. However, the jump-up frequency for both configurations lies between 26 Hz - 27 Hz. This supports the observation that the jump-up frequency is only dependent on the cubic stiffness coefficient as given in Eq. (2.4) and the jump-down frequency is a function of both the cubic stiffness coefficient and the damping as given in Eq. (2.5).

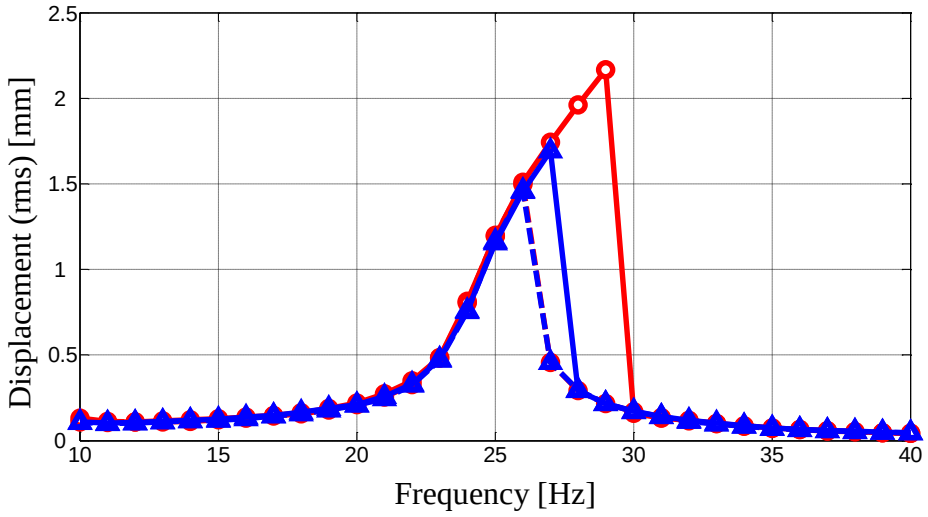

Figure 6. Measured rms displacement response for the open-circuit system: sweep-up (solid-circle), sweep-down (dashed-circle). The case of 200 Ohm load is also shown: sweep-up (solid-triangle), sweep-down (dashed-triangle).

To determine the system parameters using Eqs. (2.6) and (2.7), the jump-down frequency for the open-circuit system was taken to be 30 Hz and for the one with 200 Ohm resistance it was taken to be 28 Hz. The jump-up frequency for both systems was taken to be 27 Hz. These, of course, are only upper bounds and are chosen based on the 1 Hz frequency increment. The linear natural frequency was determined experimentally from a measurement of the transmissibility when the device was excited with a low amplitude random input displacement (0.0054 mm (rms)) so that the device was still operating in the linear region. These parameters as well as the cubic stiffness coefficient and the damping ratio calculated using the method described in the previous section, are summarised in Table 1.

Resistance [Ohm]	Jump-up freq. [Hz]	Jump-down freq. [Hz]	Linear natural freq. [Hz]	Cubic stiffness coefficient γ	Damping ratio ζ
∞ (open-circuit)	27	30	25.6	2.72×10^{-4}	0.014
200	27	28	25.6	2.72×10^{-4}	0.018

Table 1: Estimated system parameters.

Figures 7(a) and (b) show the plots of the simulated and measured responses for the open-circuit system and that with 200 Ohm resistance, respectively. Generally, the simulations and the measurements agree reasonably well. The largest errors occur between 24 Hz and 26 Hz for both configurations. This may be due to the error in estimating the jump-up and jump-down frequencies or due to the assumption that only the fundamental harmonic dominates the response with the higher harmonics being neglected (This was checked numerically, and it was found that in some frequency regions, their contributions to the responses are significant; however, these results are not presented here for brevity). It is thought that the presence of the even-order harmonics was because of the asymmetry of the system due to gravity acting on the mass rather than inherited asymmetry of the stiffness.

(a)

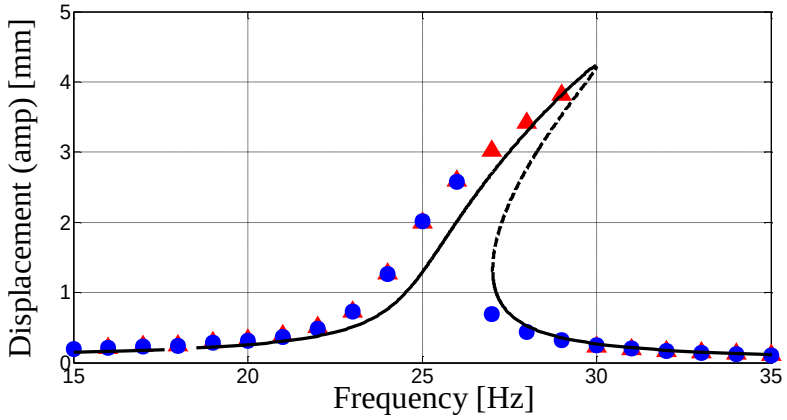

(b)

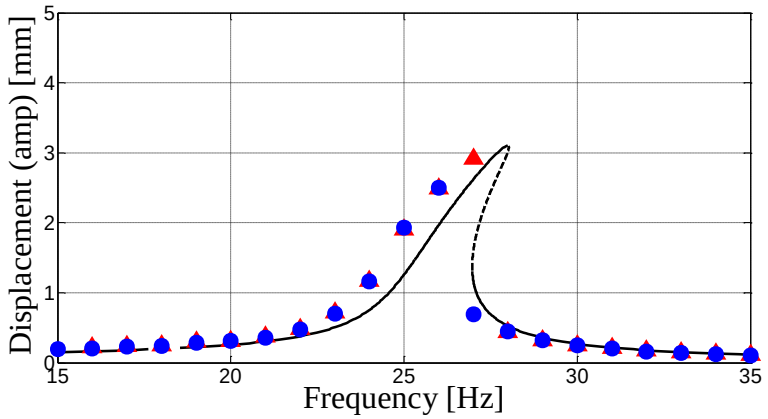

Figure 7. The simulated response (solid and dashed lines) and the measured response: red triangle (sweep-up), blue circle (sweep-down); (a) open-circuit and (b) 200 Ohm.

The estimate of the cubic stiffness coefficient using the jump-frequencies is also compared to that determined in the quasi-static measurement, which is $\gamma = k_3 Z^2 / k_1 = 2.85 \times 10^{-4}$, where $Z = 0.1\text{mm}$. Comparing this value to the one given in Table 1, it can be seen that the difference between these two estimates is approximately 5%.

The estimate of the damping ratio using the jump frequencies is shown to be accurate as well. It is calculated in three ways: using Eq. (2.7), the logarithmic

decrement method [14] and from the peak value of the transmissibility [14]. The three values are plotted in Figure 8 for several values of the load resistance. Note that the results calculated from the jump frequencies are shown only for the system with electrical resistance greater than 100 Ohm (i.e. small damping). For larger values of damping the system behaves as a linear system with no jump characteristics. Generally, it can be seen that the estimate of damping using the three methods is consistent.

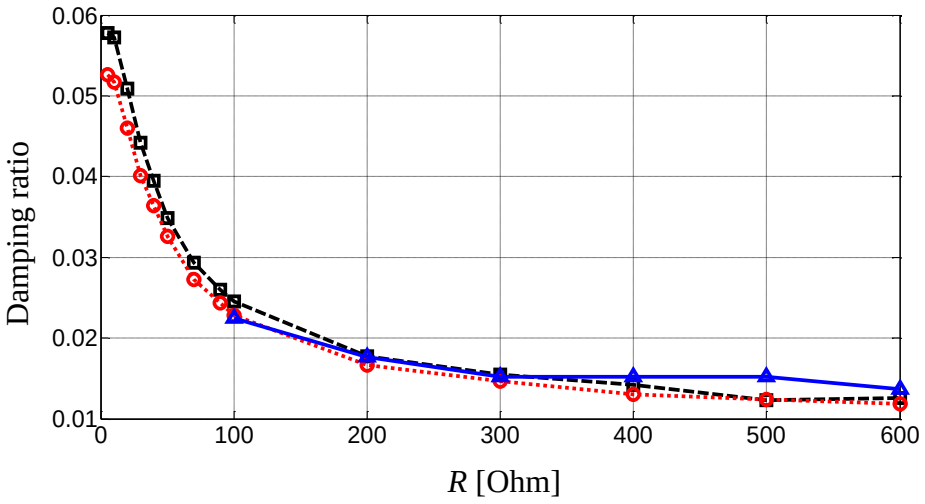

Figure 8. The estimate of the damping ratio using three different methods; logarithmic decrement method (dashed-square), peak of transmissibility (dotted-circle), and jump frequencies (solid-triangle).

3.4. Possible errors in the estimation of the non-linearity and the damping parameters

The sensitivity of the estimated cubic stiffness coefficient and the damping ratio on the jump frequencies is studied in this subsection using Eqs. (2.9) and (2.11). Due to the vertical tangency mentioned before, the true values for the jump-up and jump-down frequencies of the system with a 200 Ohm resistance are assumed to be respectively given by 27 Hz and 28 Hz.

The relative error, which may exist when the jump-up frequency deviates away from the assumed true value is shown in Figure 9. For this particular configuration, it can be seen that the error in the estimation of the cubic stiffness coefficient can be nonnegligible with small deviation from the assumed true value of the jump-up frequency. This error can be minimised by using a very small frequency increment in the search of the jump frequencies. Thus, for this method to give reliable results, the jump frequencies should as accurate as possible.

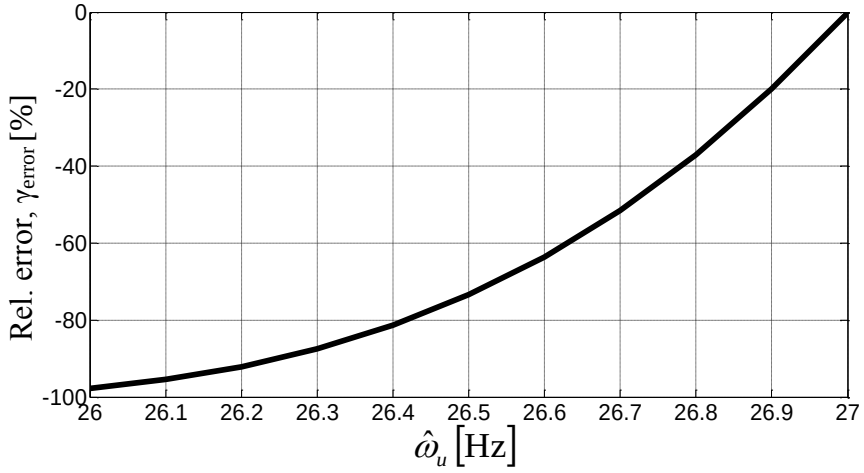

Figure 9. Relative error in the estimate of non-linearity γ with respect to the variation of the jump-up frequency from the assumed true value 27 Hz.

4. CONCLUSIONS

The jump phenomena in a Duffing oscillator are usually seen as undesirable and many techniques and control strategies have been developed to avoid them. However, in this work, the change of this perception has been proposed, showing how one can benefit from knowing the jump-up and jump-down frequencies. An experiment has been conducted on an electromagnetic device. It has been demonstrated that the estimates of the cubic stiffness coefficient measured quasi-statically and by using the method involving the jump frequencies compared well. The damping in the device has been measured using three different methods including the one involving the jump-frequencies and these also compared well. An error analysis of the proposed method showed that certain errors can be potentially incurred, but that these can be minimised by using a very small frequency increment in the determination of the jump frequencies.

REFERENCES

[1] D. Wagg, S. Neild, *Nonlinear Vibration with Control*, Springer, 2015.

[2] J. Warminski, S. Lenci, M.P. Cartmell, G. Rega, M. Wiercigroch (Eds.), *Nonlinear Dynamic Phenomena in Mechanics*, Springer, 2012.

[3] I. Kovacic, R. Rand, Straight-line backbone curve, *Communication in Non-linear Science and Numerical Simulations* 18 (2013) 2281-2288.

[4] H.J. Rice, J.R. McCraith, Practical non-linear vibration absorber design, *Journal of Sound and Vibration* 116(3) (1987) 545-559.

[5] I. Kovacic, M.J. Brennan, T.P. Waters, A study of a non-linear vibration isolator with quasi-zero stiffness characteristic, *Journal of Sound and Vibration* 315(3) (2008) 700-711.

[6] B.P. Mann, N.D. Sims, Energy harvesting from the nonlinear oscillations of magnetic levitation, *Journal of Sound and Vibration* 319(1-2) (2009) 515-530.

[7] R. Ramlan, M.J. Brennan, B.R. Mace, I. Kovacic, Potential benefits of a non-linear stiffness in an energy harvesting device, *Nonlinear Dynamics* 59 (2010) 545-558.

[8] M. Younis, *MEMS: Linear and Nonlinear Statics and Dynamics*, Springer, 2011.

[9] I. Kovacic, M.J. Brennan, *The Duffing Equation: Nonlinear Oscillators and their Behaviour*, John Wiley & Sons, 2011.

[10] M.J. Brennan, I. Kovacic, A. Carella, T.P. Waters, On the jump-up and jump-down frequencies of the Duffing oscillator, *Journal of Sound and Vibration* 318(4-5) (2008) 1250-1261.

[11] B. Tang, M.J. Brennan, V. Lopes Jr, S. da Silva, R. Ramlan, Using nonlinear jumps to estimate cubic stiffness nonlinearity: An experimental study, *Journal of Mechanical Engineering Science, Proceedings of the Institution of Mechanical Engineers Part C*, DOI: 10.1177/0954406215606746, in press.

[12] R. Ramlan, M.J. Brennan, B. Mace, I. Kovacic, S. Burrow, On the estimation of linear viscous damping in the Duffing oscillator, *The Sixteenth International Congress on Sound and Vibration*, Kraków, Poland, 5–9 July, 2009, Vol. 2, pp. 1088-1095.

[13] R. Ramlan, M.J. Brennan, B.R. Mace, S. Burrow, On the performance of a dual-mode non-linear vibration energy harvesting device, *Journal of Intelligent Material Systems and Structures* 23 (2012) 1423-1432.

[14] S.S. Rao, *Mechanical Vibrations*, Addison-Wesley Pubs, 2nd Ed., 1990.